J Therm Anal Calorim (2009) 98:19–28
DOI 10.1007/s10973-009-0229-7

Interaction of an anticancer drug, gemcitabine, with phospholipid bilayers

Barbara Pili · Claudie Bourgaux · Florian Meneau · Patrick Couvreur · Michel Ollivon

Special Chapter dedicated to the memory of dr. Michel Ollivon

Abstract The molecular interaction between gemcitabine, an anticancer pyrimidine analogue, and fully hydrated phospholipid (1,2-dipalmitoyl-sn-3-phosphatidylcholine, DPPC) membrane model has been investigated by Differential Scanning Calorimetry (DSC) and Small and Wide Angle X-ray Diffraction (SWAXS). The behaviour of the charged and uncharged forms of gemcitabine has been examined. Our results show that: (1) at physiological pH, gemcitabine does not modify significantly the thermal and structural properties of DPPC, (2) at pH of 2.4 the drug interacts electrostatically with the polar headgroups, inducing the formation of unilamellar vesicles and (3) at acidic pH the DPPC lamellar phase is recovered when salt is added.

Keywords Differential scanning calorimetry (DSC) · Gemcitabine · pH · DPPC · X-ray diffraction (SAXS-WAXS)

Introduction

Gemcitabine (2′,2′-difluoro-2′-deoxycytidine, dFdC) is a fluorinated nucleoside analogue with antineoplastic activity against a wide range of solid tumours including lung, pancreatic, bladder and breast cancers. However, gemcitabine suffers from certain drawbacks including a short plasma half-life due to deamination into the inactive difluorouracil and the induction of drug resistance.

B. Pili · C. Bourgaux (✉) · P. Couvreur · M. Ollivon
Université Paris-Sud XI, UMR CNRS 8612, 5 rue J.B.Clément, 92290 Châtenay-Malabry, France
e-mail: claudie.bourgaux@u-psud.fr

F. Meneau
Synchrotron SOLEIL, L'Orme des Merisiers, Saint-Aubin, BP 48, 91192 Gif-sur-Yvette, France

Liposomal formulations have been developed with the aim of improving the therapeutic activity of gemcitabine. Liposomes are vesicles formed by polar lipid bilayers in aqueous solvents. Due to their structural properties they are able to encapsulate either hydrophilic drugs in their aqueous core or lipophilic drugs within the bilayer. Amphiphilic molecules may reside in the interfacial region or insert in the bilayer with their hydrophilic moiety protruding in the aqueous medium.

Various effects may contribute to the better anticancer activity of the water-soluble gemcitabine when carried by phospholipid vesicles. Liposomes may provide protection against rapid metabolic inactivation of the drug, while long-circulating liposomes may allow a passive targeting to certain tumours by the so-called enhanced permeability and retention (EPR) effect. Indeed, the leaky vasculature of some solid tumours in combination with impaired lymphatic drainage may induce an efficient extravasation and a selective accumulation of small colloidal carriers (<200 nm) into tumours. Consequently, the extent of accumulation in healthy tissues and toxicity may be reduced. Liposomes might also improve the drug uptake by cancer cells either by endocytosis of liposomes or by fusion of the outer liposomal bilayer with the cell membrane.

In fact, in vitro and in vivo experiments have confirmed the potential of liposomes in improving gemcitabine efficacy. The serum half-life of gemcitabine was extended from 0.15 to 13.3 h when entrapped in egg phosphatidylcholine/cholesterol (EPC/chol 1/1 molar ratio) liposomes of 60–80 nm mean diameter. Furthermore, an increased anticancer activity with respect to free gemcitabine was demonstrated in two human tumour xenograft models, the subcutaneously growing soft tissue sarcoma SXF 1301 and the orthotopically growing bladder cancer BXF 1299T. This enhanced in vivo efficacy was explained by the sustained release of

gemcitabine and by the above mentioned EPR effect. In these experiments the reticuloendothelial (RES) system was probably rapidly saturated by a fraction of the high number of injected liposomes, so that the remaining liposomes had long circulation lifetime [1]. A similar liposomal formulation of gemcitabine (hydrogenated EPC/chol 55/45 molar ratio) showed also promising antitumoural activity against MIA PaCa-2, a pancreatic carcinoma, growing orthotopically in nude mice [2]. Entrapment of gemcitabine in vesicles was also found to influence its in vitro cytotoxicity. After an incubation of 48 h free gemcitabine did not display cytotoxic effect on Caco-2 colon carcinoma cells. In contrast, gemcitabine-loaded liposomes exhibited dose-dependent cytotoxicity. This improvement of anticancer activity was correlated to the intracellular levels of the drug. It has been observed that cell penetration properties could be modulated by the lipid composition of vesicles. Higher intracellular levels were achieved using pegylated liposomes made from a mixture of dipalmitoylphosphatidylcholine (DPPC) and cholesterol [3]. The respective effects of free gemcitabine and pegylated gemcitabine-loaded liposomes were also compared in vitro on ARO cells, a human anaplastic thyroid carcinoma. The liposomal formulation noticeably improved the cytotoxicity of gemcitabine, suggesting again the ability of liposomes to promote the intracellular drug uptake [4, 5].

These results have emphasized the potential interest of liposomal formulations of gemcitabine. The first requirement in using liposomes as drug delivery devices is to achieve an efficient trapping and retention of the drug. Despite its two fluorine atoms gemcitabine is much more soluble in water than in oil. Therefore, this compound is expected to be mainly trapped in the liposome aqueous core. However, interactions between the drug and the lipid vesicles may modulate the encapsulation efficiency and release profile. The aim of this study was to characterize the interactions between gemcitabine and DPPC, a lipid used in most liposomal formulations. Furthermore, DPPC bilayers may also be considered as a simple model of target biomembrane. Any interaction would lead to a modification of the thermal and structural parameters of the lipid phase. The influence of gemcitabine on DPPC bilayers has thus been investigated using Differential Scanning Calorimetry (DSC) and Small and Wide-Angle X-ray Scattering (SWAXS).

Materials and methods

Materials

1,2-dipalmitoyl-sn-3-phosphatidylcholine (DPPC) (molecular weight of 733.56, purity 99%) was purchased from Avanti Polar Lipids (Alabaster, Alabama, USA) and used without further purification.

Fig. 1 Chemical structure of gemcitabine (dFdC)

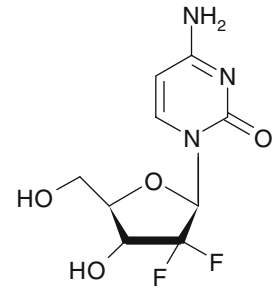

Gemcitabine hydrochloride (2′-deoxy-2′,2′-difluorocytidine monohydrochloride, $C_9H_{11}F_2N_3O_4{\cdot}HCl$, β-isomer, dFdC, Fig. 1) was purchased from Sequoia Research Products (Pangbourne, UK). dFdC is a hydrophilic molecule (molecular weight of 299.66) soluble in water and almost insoluble in polar organic solvents. dFdC has a low partition coefficient ($K_{ow} = 0.05$). The pH obtained upon dissolution of gemcitabine hydrochloride ranges between 2.7 and 3.3 [6]. Its solubility in water is limited to 40 mg/mL. dFdC solubility decreases with increasing pH, so that its solubility is about 15.5 mg/mL between pH 5 and pH 9 [7].

NaOH pellets (molecular weight of 40.00) were obtained from Prolabo (West Chester, Pennsylvania, USA), and saline solution (NaCl, molecular weight of 58.44, 154 mM) was purchased from Aguettant (Lyon, France).

Purified water (Milli-Q, Waters) was used for sample and buffer preparations.

Sample preparation

Samples (about 20 mg of anhydrous lipids) were prepared by dissolving dry lipid powders in chloroform. The solvent was removed under a nitrogen stream followed by drying under vacuum at 4 °C for 12 h.

Acidic dFdC·HCl solution (dFdC·HCl 35 mM) was neutralized with a sodium hydroxide solution (1 M) to obtain a pH of 6.9 and buffered with Hepes (10 mM). Dry films were fully hydrated (80%) with this solution so that the final concentration of DPPC was about 250 mM.

Dry films were also hydrated in excess (water 87%) with acidic dFdC solutions, with or without added salt. The concentration of gemcitabine ranged between 24 and 120 mM. The pH of all these solutions was set to 2.4 and the final concentration of DPPC was 227 mM.

The suspensions were heated above the chain melting transition temperature of DPPC and vortexed in order to ensure good homogeneity. They were allowed to equilibrate during 24 h.

An aliquot of the samples (about 10 mg) was loaded into DSC hermetically sealed aluminium pans (50 µL, Perkin-Elmer, Waltham, Massachusetts, USA) and quartz capillaries (external diameter 1.4 ± 0.1 mm and wall

thickness 0.01 mm) (Glas, Müller, Berlin, Germany). When necessary, low-speed centrifugation (<1,000 rpm) was used to concentrate the lipidic phase down to the bottom of the capillary. The top of the capillary was closed by a drop of paraffin to prevent water evaporation. Before analysis, DSC pans and capillaries were kept at 4 °C for durations comprised between 1 night and 1 week.

Differential scanning calorimetry

Thermal analysis has been carried out using a DSC 7 (Perkin-Elmer, Inc.) equipped with a cooling device (Intracooler II) in dry air atmosphere. The instrument was standardized using the enthalpy and melting point of lauric acid (99.5% purity, $T_m = 43.7$ °C, $\Delta H_m = 35.713$ kJ/mol) [8].

Data analysis was performed using TA Universal Analysis program (New Castle, Delaware, USA). The transition temperatures were taken at the onset of the transitions (T_{onset}) i.e. the intersection of the tangent to the left side of the endothermic peak with the baseline and at the peak maximum (T_p). For the main transition the offset temperature (T_{offset}), corresponding to the completion of transition, was also reported. This temperature was taken at the intercept of the baseline with the tangent to the right side of the heating curve.

The enthalpy of the transitions was obtained from the area under the peaks and normalized by the phospholipid content. To calculate the area under the peak a baseline connecting the linear segments of the heat capacity curve between the onset and endpoint of the transition was subtracted.

X-ray diffraction

X-ray scattering experiments were performed on the Austrian SAXS beamline at ELETTRA [9, 10] and on the SWING synchrotron beamline at SOLEIL. Samples were thermostated in a laboratory made microcalorimeter, Microcalix [11, 12]. On the ELETTRA beamline small (SAXS) and wide angle (WAXS) X-ray scattering patterns were recorded simultaneously using two position-sensitive linear gas detectors filled with an argon–ethane mixture. On the SWING beamline X-ray patterns were recorded by a two-dimensional CCD detector. The scattered intensity are reported as a function of the scattering vector $q = 4\pi\sin\theta/\lambda$, where 2θ is the scattering angle and λ the wavelength. The calibration of the q-range was carried out using pure tristearine (2Lβ form) [13] and silver behenate [14]. Sample-to-detector distance and beam energy were chosen to cover the required q-range. In the case of dilute unilamellar vesicles the scattered intensity from a capillary filled with water was subtracted after normalization from the sample scattering curves.

Results and discussion

In excess water the zwitterionic molecules of DPPC spontaneously form bilayers whose structure and long-range organisation depend on temperature. As temperature is increased from room temperature, DPPC is known to display successively three lamellar phases, the gel phase $L_{\beta'}$, the gel ripple phase $P_{\beta'}$ and, finally, the liquid-crystalline phase L_α. The influence on DPPC bilayers of uncharged gemcitabine, at neutral pH, and of positively charged gemcitabine, at acidic pH, has been investigated using DSC and SAXS and WAXS. DSC monitored the temperature and enthalpy of transitions between the different structures while X-ray diffraction patterns at small and wide angles yielded information respectively on long range bilayer organisation and hydrocarbon chain packing within these supramolecular assemblies.

Interactions between gemcitabine and DPPC bilayers at neutral pH

The pH of aqueous solutions of gemcitabine hydrochloride was increased to 6.9 with NaOH and buffered with 10 mM HEPES. Gemcitabine solubility being limited to about 15 mg/mL in the pH range 5–9, DPPC bilayers were fully hydrated at neutral pH with a 35 mM solution of gemcitabine. Since the reported pK_a value for the amino group of gemcitabine is 3.58, gemcitabine was expected to be predominantly in the unprotonated form.

As shown in Fig. 2 the DSC curve obtained for DPPC hydrated with gemcitabine solution is similar to that of DPPC in excess water recorded at the same heating rate of 5 °C/min. The weak $L_{\beta'}$ to $P_{\beta'}$ pretransition is followed by the sharp endothermic $P_{\beta'}$ to L_α main transition. The onset temperature of the pretransition decreases from 35.9 to 34.1 °C and its enthalpy, $\Delta H_p = 5$ kJ/mol of DPPC, is a little smaller than that of DPPC (5.4 kJ/mol). The main transition occurs at a T_{onset} of 41.4 °C with an enthalpy of 36.7 kJ/mol of DPPC. These values are nearly the same as those of DPPC [15] and are maintained after at least a week of incubation. The cooperativity of the transition, inferred from the width of the endotherm is not affected. The enthalpy of the main transition arises mainly from trans/gauche rotational isomerization of chains and volume expansion associated to melting of the hydrocarbon lipid chains, it is thus sensitive to the presence of host molecules inserted between chains [16]. The absence of significant variation of ΔH suggests that gemcitabine is not embedded into bilayers. On the other hand, the slight change in the pretransition is an indication in favour of weak interactions between gemcitabine and the polar headgroups.

The influence of neutral gemcitabine on DPPC has been further investigated by means of X-ray diffraction.

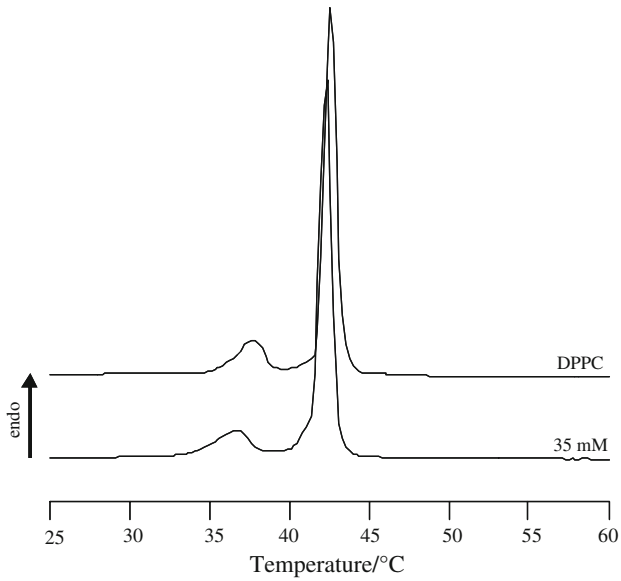

Fig. 2 DSC curves of DPPC fully hydrated with either water or a 35 mM dFdC solution (pH 6.9). Curves were recorded upon heating at 5 °C/min

Figure 3 displays SAXS and WAXS intensity profiles of DPPC hydrated either with water or with gemcitabine solution. They were recorded at 20 °C, below the pre-transition, and at 50 °C, above the main transition. These patterns are characteristic respectively of the $L_{\beta'}$ gel phase and of the L_{α} fluid phase. SAXS patterns exhibit equidistant peaks indicative of lamellar phases. Note that fewer orders of diffraction are observed for fluid phases due to suppression of higher orders by Helfrich fluctuations. In the presence of gemcitabine the lamellar spacing, deduced from the position of the peaks, decreases slightly from 63.4 to 62.8 Å in the gel phase and from 65.8 to 63.1 Å in the fluid phase. The most obvious change induced by gemcitabine is the broadening of the SAXS peaks for both phases. The coherence length of the lamellar stacks may become smaller, and/or which is more likely, the distribution of repeat distances become wider as gemcitabine is added. WAXS patterns of DPPC either in water or in drug solution are identical. At 20 °C they both display a narrow peak at $q = 1.48$ Å^{-1} ($d = 4.3$ Å) along with a shoulder at about $q = 1.51$ Å^{-1} ($d = 4.2$ Å), attributed respectively to the (2,0) and (1,1) reflections of a face-centered rectangular lattice. Fully extended hydrocarbon chains are packed in a quasi-hexagonal lattice, chains are tilted with respect to the plane of the bilayer. In the fluid phase a small broad bump centered at about 1.4 Å^{-1} ($d = 4.5$ Å) is observed. Chains have a highly disordered, liquid-like conformation [17–22].

Taken together, calorimetric and structural data indicate that gemcitabine does not penetrate DPPC membranes nor modify significantly the balance of attractive and repulsive forces between bilayers. Gemcitabine, which is a water-soluble molecule uncharged at neutral pH, seems to weakly interact with polar headgroups, probably through hydrogen bonding.

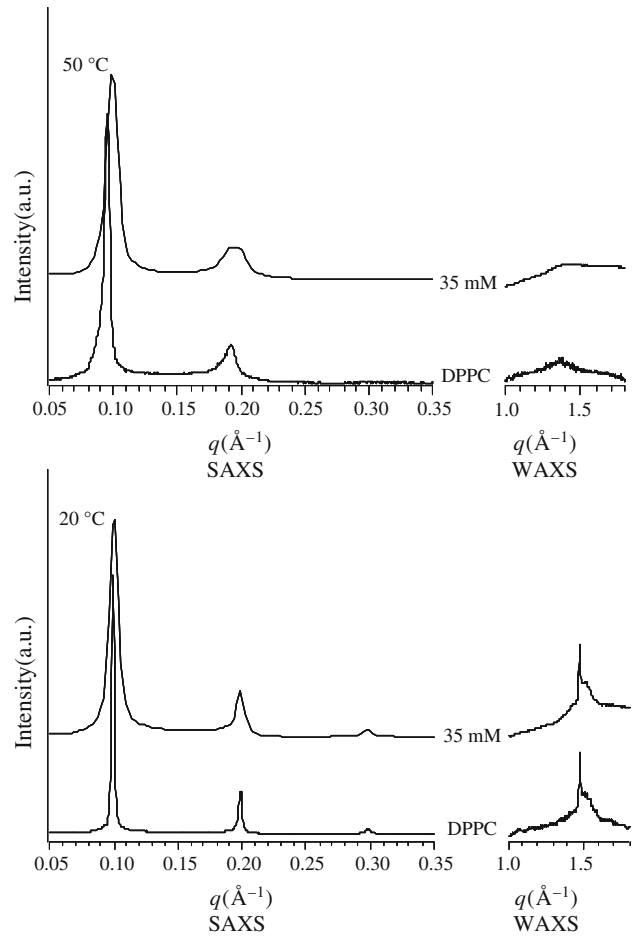

Fig. 3 X-ray diffraction patterns (SAXS and WAXS), at 20 and 50 °C, of DPPC in water and in a 35 mM dFdC solution (pH 6.9)

Interactions between gemcitabine and DPPC bilayers at acidic pH

In a second set of experiments, DPPC bilayers have been hydrated with aqueous solutions of gemcitabine hydrochloride and stored at 4 °C for durations comprised between 1 night and 1 week. Gemcitabine solubility increases up to about 38 mg/mL at low pH so that the effect of drug could be examined in a large range of concentration, namely between 15 and 120 mM. The pH of these solutions was set to 2.4. It is likely that a large fraction of gemcitabine molecules was protonated in these solutions.

The DSC curves and SAXS and WAXS patterns of DPPC hydrated with acidic solutions of gemcitabine have been recorded and compared to those of DPPC in water acidified to pH 2.4 with HCl. It was first checked that protonation of phosphate groups at this low pH was too

weak to have a significant effect on the transitions and organisation of the DPPC bilayers. The temperatures of the transitions are not modified and the lamellar order is preserved with the same repeat distances.

DSC curves of DPPC obtained after an incubation of 24 h and 48 h in the presence of different concentrations of gemcitabine are reported in Fig. 4. We focus first on samples allowed to equilibrate during 48 h. The drug presence influences the thermodynamic parameters of DPPC transitions in a concentration-dependent manner. The pretransition progressively vanishes upon increasing gemcitabine concentration. At gemcitabine concentration greater than 40 mM the pretransition is too weak and too broad to be monitored. The main transition becomes broader, indicating a decrease of cooperativity. Its maximum is shifted to a slightly higher temperature while the onset temperature is not affected. A shoulder appears on the high-temperature side of the peak for concentrations higher than 25 mM. The DSC signal evolves progressively towards a wide split endotherm whose second component shifts gradually to higher temperature and increases at the expense of the first with increasing gemcitabine content. At high gemcitabine concentrations the second endotherm takes place about 4 °C above the first. Split endotherms are also observed in the second heating scan (data not shown).

It is worth noting that the total enthalpy, deduced from integration of peak areas between the onset and the offset of the endothermic event, does not depend on gemcitabine concentration (Table 1). This suggests that this broad transition range corresponds to conversion of the gel phase into fluid phase of DPPC. At high gemcitabine concentration the two peaks of split endotherms likely represent two populations of phospholipid molecules undergoing chain melting at different temperatures. It may be assumed that micro-heterogeneous distribution of gemcitabine interacting with DPPC lead to formation of lateral domains. The first peak would correspond to gemcitabine-depleted domains while the second peak (or shoulder) at higher temperature should arise from gemcitabine-rich domains. The absence of significant variation in ΔH suggests that gemcitabine does not insert in the hydrophobic core of the bilayer. Gemcitabine, which carries a positive charge, could interact electrostatically with the negatively charged phosphate group of DPPC and adsorb at the lipid–water interface. Water molecules may be involved in the interactions between ions and lipid polar groups or direct ion–lipid interactions may result in the displacement of their water of hydration. It may be hypothesized that association between the phosphate group and gemcitabine induces a partial release of their water of hydration. It is a well established result that hydrophilicity of phospholipids originates mainly from the phosphate and carbonyl groups and that partial dehydration of the polar headgroup, for example upon binding of cations, tends to raise the melting temperature [23–25]. The occurrence of a second endotherm at higher temperature in the presence of gemcitabine may be tentatively explained in this way.

It should be emphasized that association of gemcitabine to the bilayers seemed to proceed gradually. DSC recordings have been performed after an incubation of 24, 48 h and 7 days of DPPC in the drug solution. At short incubation time

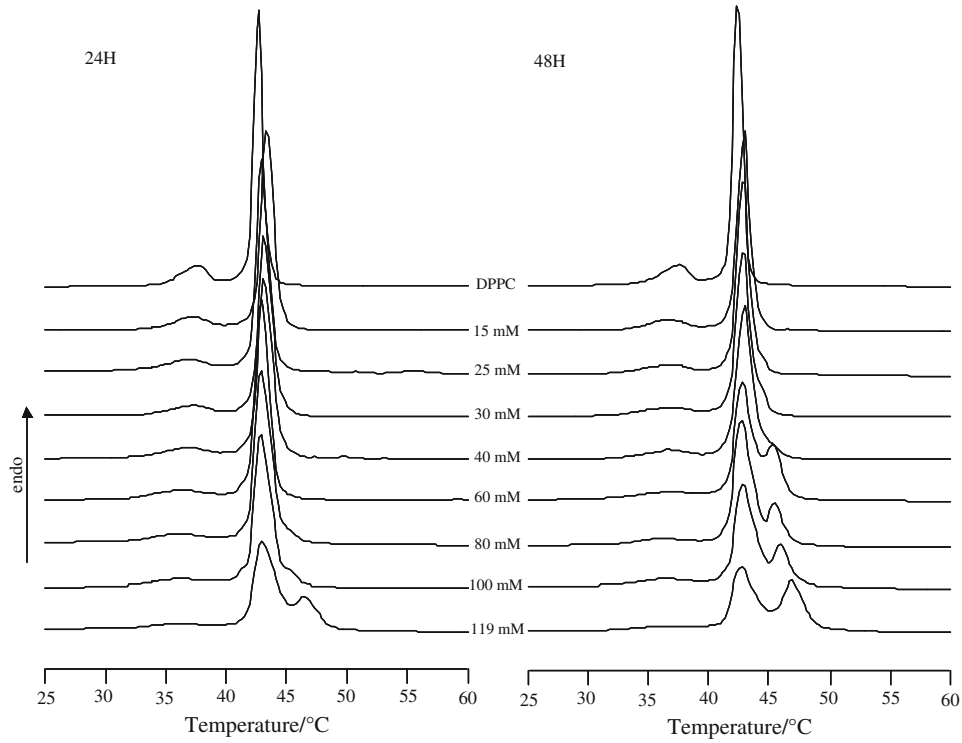

Fig. 4 DSC curves of DPPC fully hydrated with dFdC solutions, as a function of dFdC concentration (pH 2.4). The dFdC concentration is indicated for each curve. Curves were recorded at 5 °C/min, 24 or 48 h after hydration

Table 1 Thermodynamic data determined by DSC 24 and 48 h after hydration of DPPC with dFdC solutions (pH 2.4)

dFdC (mM)	24 h						48 h					
	$T_p$onset/°C	T_p/°C	ΔH_p/kJ/mol	$T_m$onset/°C	$T_m$offset/°C	ΔH_m/kJ/mol	$T_p$onset/°C	T_p/°C	ΔH_p/kJ/mol	$T_m$onset/°C	$T_m$offset/°C	ΔH_m/kJ/mol
0	35.1	37.7	5.1	41.8	43.4	40.4	34.8	37.5	5.3	41.6	43.2	40.2
15	34.7	37.1	3.9	42.4	44.4	38.5	33.7	36.3	3.4	41.8	44.0	38.4
25	34.1	36.7	3.0	42.0	44.1	38.6	32.9	36.7	2.8	41.8	44.0	37.9
30	34.1	37.1	2.8	42.2	44.3	37.0	32.7	36.5	2.4	41.7	45.1	36.4
40	33.3	36.7	3.0	42.1	44.4	42.5				41.8	46.2	38.6
60				41.8	44.0	43.0				41.6	46.7	42.3
80				41.8	44.5	40.4				41.6	46.8	41.8
100				41.8	46.4	38.3				41.6	47.4	38.4
119				41.7	48.4	37.8				39.4	48.8	35.9

(24 h), the main endotherm is narrower and the second endotherm is not detected at gemcitabine concentration lower than 120 mM (Fig. 4). As evidenced by curves recorded after an incubation of 7 days, samples did not significantly evolved between 48 h and 7 days (data not shown). Increasing incubation time appears equivalent to increase the concentration of gemcitabine in water. Gemcitabine might penetrate progressively between the polar headgroups and bind to phosphate groups until an equilibrium partition between the aqueous and lipid phases is reached.

X-ray experiments have been performed to get a better insight into the influence of gemcitabine on the structure of DPPC (Fig. 5). In the gel phase WAXS patterns are less asymmetric in the presence of gemcitabine, the intensity and peakedness of the shoulder at $q = 1.54$ Å^{-1} increase and become similar to those of the peak at $q = 1.46$ Å^{-1}. Upon samples heating WAXS peaks disappeared in agreement with DSC results. On the other hand, SAXS experiments revealed the disappearance of the smectic order of DPPC bilayers, both in the gel phase, at 20 °C and in the fluid phase, at 50 °C. Whatever the concentration of

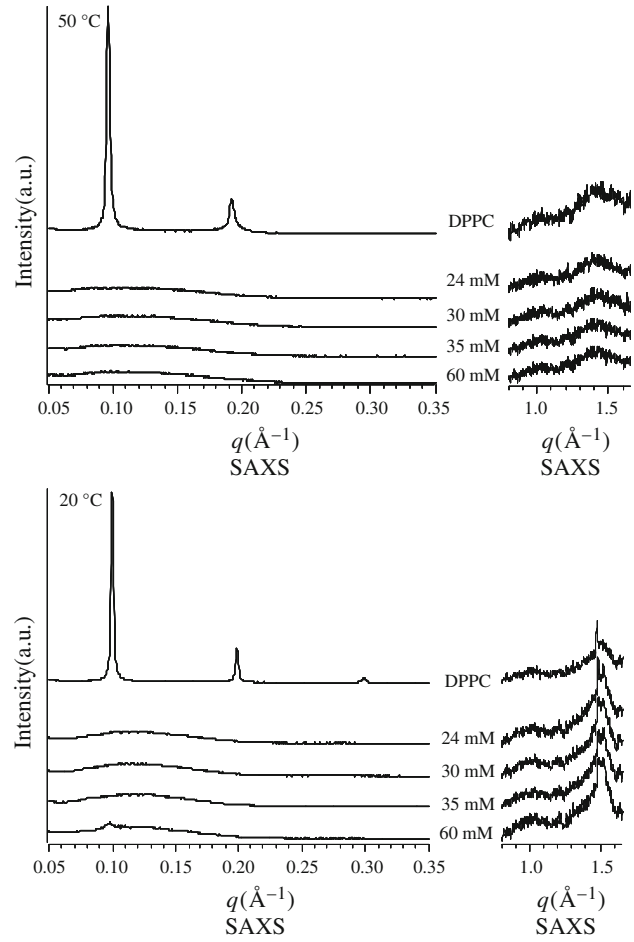

Fig. 5 X-ray diffraction patterns (SAXS and WAXS), at 20 and 50 °C, of DPPC in dFdC solutions as a function of dFdC concentration (pH 2.4). The dFdC concentration is indicated for each curve

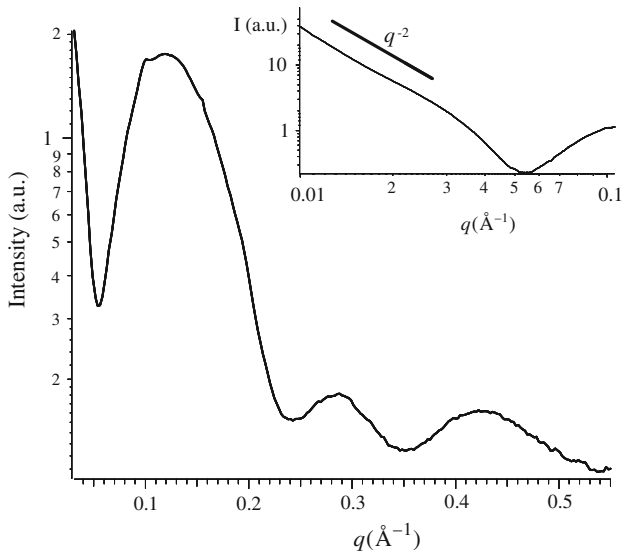

Fig. 6 SAXS pattern at 20 °C of DPPC in a 35 mM dFdC solution (pH 2.4), indicative of unilamellar vesicles. Two sample-to-detector distances and energies were used: 56 cm, 15 keV and 5.6 m, 11 keV (insert). At low q the intensity exhibits a q-2 dependence characteristic of planar membranes (insert)

gemcitabine in the range 20–60 mM, only diffuse scattering is observed (broad bump at $q \sim 0.12$ Å^{-1}). The same profile is evidenced for 120 mM gemcitabine solution (data not shown). These patterns suggest the presence of unilamellar or oligolamellar vesicles. This was confirmed by analysis of the SAXS curves measured over an extended q-range, namely between 0.01 and 0.55 Å^{-1}. The scattering curve shown in Fig. 6 may be described in terms of the form factor of a bilayer. Indeed, in the range $q = 0.014$–0.025 Å^{-1}, the log I–log q plot clearly exhibits a linear variation with a slope of approximately 2, as expected for planar membrane (Porod regime). At higher q the scattering intensity is characterized by periodic oscillations arising from the bilayer thickness. Note that Bragg peaks typical of multilamellar vesicles are not observed.

The formation of unilamellar vesicles could be explained by binding of gemcitabine to phosphate group, imparting a net positive charge to bilayers and thus inducing an electrostatic repulsion between them. Charged phospholipid bilayers are known to swell continuously with increasing water content when electrostatic repulsion overwhelms Van der Waals attraction. Above a certain threshold disruption of lamellar stacks may lead to formation of unilamellar vesicles. At low ionic strength of the solution spontaneous vesiculation may occur even at relatively low surface charge density of the bilayers if lipid dilution is sufficient. It has been previously found that neutral bilayers doped with only a few percent of a charged lipid or detergent or with adsorbed ions may exhibit this behaviour [26–28].

Interactions between gemcitabine and DPPC bilayers at acidic pH with added salt

Finally, DPPC has been hydrated with acidic solutions of gemcitabine containing 154 mM NaCl (pH 2.4). The DSC curves recorded 48 h after hydration show the same trends as those of DPPC in gemcitabine solutions without added salt (Fig. 7). As gemcitabine content increases, the

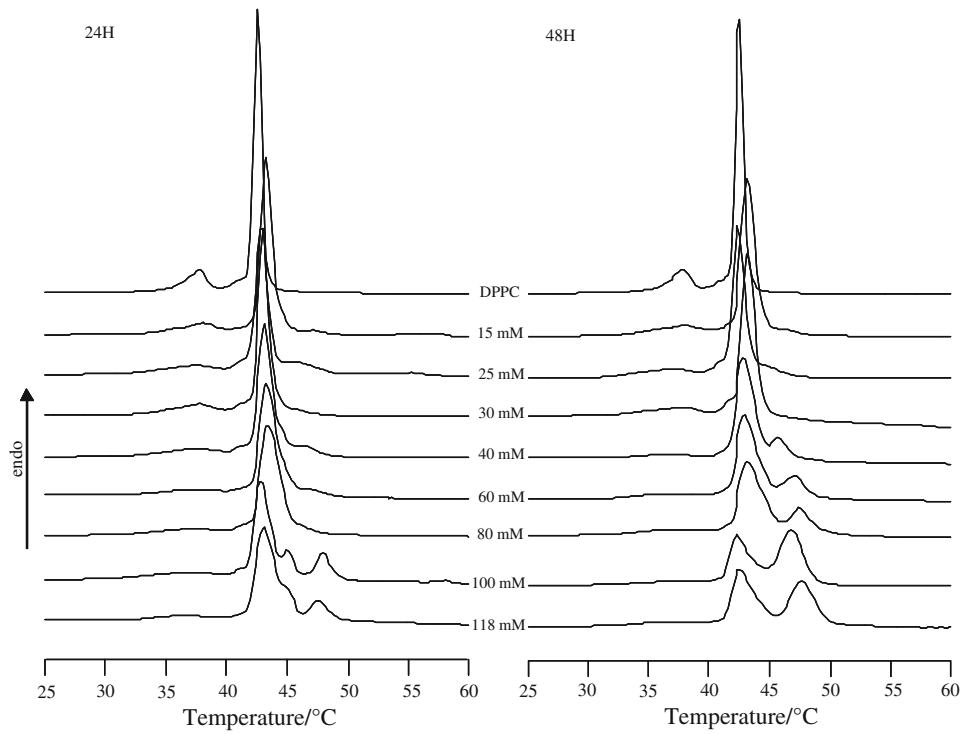

Fig. 7 DSC curves of DPPC fully hydrated with dFdC solutions containing 154 mM NaCl, as a function of dFdC concentration (pH 2.4). The dFdC concentration is indicated for each curve. Curves were recorded at 5 °C/min, 24 and 48 h after hydration

pretransition progressively disappears while the main transition broadens and evolves to yield two separated endotherms, suggesting again that gemcitabine-poor and gemcitabine-rich domains coexist. The total enthalpy associated with both peaks is nearly independent of gemcitabine concentration and is a little smaller than without NaCl (Table 2). The evolution of DSC curves as a function of incubation time is consistent with a gradual adsorption of gemcitabine in the interfacial region. The binding of gemcitabine increases during the first 48 h and then remains stable for at least 1 week. Note that addition of NaCl seems to enhance slightly the affinity of gemcitabine for DPPC since the high-temperature component of the main transition is more pronounced in the concentration range 40–120 mM.

In strong contrast, addition of NaCl markedly modifies the long-range organisation of DPPC bilayers. Unilamellar vesicles are no longer observed. The multilamellar structure is recovered both in the gel and the fluid phases as revealed by typical SAXS reflections. This is attributed to the screening of surface charges, due to gemcitabine adsorption, by ions in solution. The Debye screening length λ_D, which corresponds to the thickness of the diffuse double layer depends on the ionic strength of the solution. For a 154 mM NaCl solution λ_D is $\sim$10 Å. As λ_D is smaller than the distance between membranes, estimated to be about 25 Å for DPPC in the fluid phase hydrated with water [29], the electrostatic repulsion, which decays exponentially, should be very weak. In this case the DPPC lamellar phases show only limited swelling and may coexist with excess water. In the gel phase equilibrium spacing is expected to result mainly from the balance of attractive Van der Waals interactions and repulsive hydration interactions. In the fluid phase there is an additional steric repulsion due to bilayer undulations (Helfrich forces). Figure 8 exhibits the SAXS and WAXS profiles of DPPC in a 39 mM solution of gemcitabine with added salt, the corresponding profiles of DPPC in an acidic aqueous solution with added salt are also displayed for comparison. In the gel phase, at 20 °C, only a slight increase of the lamellar spacing from 63.1 to 63.9 Å is observed in the presence of gemcitabine, confirming the screening of the electrostatic interactions. Bragg reflections at small angles are broader, pointing to a stacking disorder of the bilayers. In the fluid phase the first- and second-order small-angle reflections are split. A shoulder appears on the high-q range of the first-order peak at $q = 0.094$ Å^{-1} (66.9 Å). This is most likely due to a nonhomogeneous distribution of gemcitabine at the lipid- water interface, leading to slightly different interlamellar distances. However, the mean lamellar spacing is almost the same as that of pure DPPC. WAXS patterns are not affected by the presence of gemcitabine.

Table 2 Thermodynamic data determined by DSC 24 and 48 h after hydration of DPPC with dFdC solutions containing 154 mM NaCl (pH 2.4)

dFdC (mM)	24 h						48 h				
	$T_p$onset/°C	T_p/°C	ΔH_p/kJ/mol	$T_m$onset/°C	$T_m$offset/°C	ΔH_m/kJ/mol	$T_p$onset/°C	T_p/°C	ΔH_p/kJ/mol	$T_m$onset/°C	$T_m$offset/°C
0	35.8	37.7	5.1	41.8	43.2	37.8	36.2	37.9	4.5	41.7	43.1
15	34.6	38.1	3.7	42.2	44.2	36.1	34.6	37.9	3.4	42.0	44.5
25	32.8	37.3	2.6	41.8	47.7	33.6	32.3	36.7	2.5	41.4	46.2
30	34.3	37.7	3.2	42.1	47.2	35.4	32.6	37.9	3.5	42.2	44.2
40	34.2	37.3	2.0	42.0	47.9	33.8				41.6	47.2
60				42.1	47.9	33.9				41.7	48.7
80				42.1	47.0	34.2				41.8	49.3
100				41.8	49.3	32.4				41.1	48.8
118				41.8	48.5	37.2				41.3	49.7

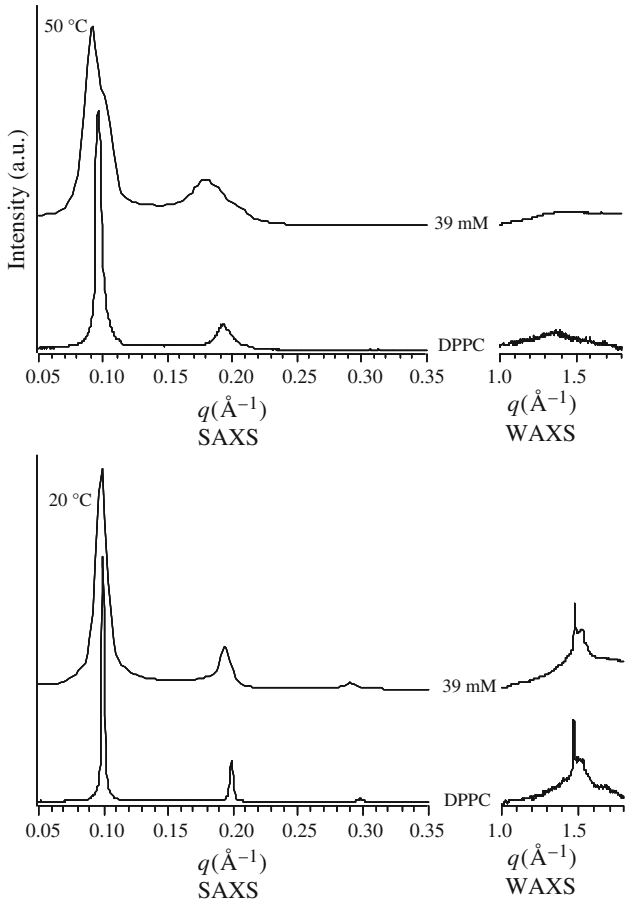

Fig. 8 X-ray diffraction patterns (SAXS and WAXS), at 20 and 50 °C, of DPPC in a 39 mM dFdC solution with added salt

Conclusions

Interactions of gemcitabine with DPPC lamellar phases have been investigated at neutral and acidic pH by DSC and X-ray diffraction. Water soluble gemcitabine partitions between the lipid interfacial region and the aqueous medium. Partition in DPPC bilayers of the protonated and unprotonated species strongly differs. At physiological pH gemcitabine, which is uncharged interacts weakly with DPPC bilayers, most probably through hydrogen bonding. The thermal and structural properties of DPPC are barely perturbed. Gemcitabine should thus locate mainly in the aqueous phase. On the contrary, at low pH the protonated form of gemcitabine could interact electrostatically with the negatively charged phosphate group of DPPC and therefore bind more tightly to the lipid interfacial region. Desorption from and permeation through liposomal bilayers might be hampered by these interactions. As a consequence, acidic pH of the vesicles aqueous core and lipids containing negatively charged groups would lead to higher trapping efficiency and better stability of liposomal formulations. Moreover the solubility of gemcitabine in water is three times higher at low pH than at neutral pH. Regarding the gemcitabine uptake by cells, results at physiological pH seem consistent with the current knowledge of gemcitabine transport. Indeed, active transport process involving specific nucleoside transporters is required for intracellular drug uptake.

Acknowledgements The authors wish to thank Dr. Sinda Lepêtre-Mouelhi and Dr. Didier Desmaele for providing the gemcitabine, Dr. Heinz Amenitsch for his support during the X-ray measurements on the Austrian SAXS beamline at the synchrotron ELETTRA (Trieste, Italy) and Enguerrand Habran for his help during experiments.

References

1. Moog R, Burger AM, Brandl M, Schuler J, Schubert R, Unger C, et al. Change in pharmacokinetic and pharmacodynamic behavior of gemcitabine in human tumor xenografts entrapment in vesicular phospholipid gels. Cancer Chemother Pharmacol. 2002;49: 356–66.
2. Bornmann C, Graeser R, Esser N, Ziroli V, Jantscheff P, Kerck T, et al. A new liposomal formulation of gemcitabine is active in an orthotopic mouse model of pancreatic cancer accessible to bioluminescence imaging. Cancer Chemother Pharmacol. 2008;61: 395–405.
3. Calvagno MG, Celia C, Paolino D, Cosco D, Iannone M, Castelli F, et al. Effects of lipid composition and preparation conditions on physical-chemical properties, technological parameters and in vitro biological activity of gemcitabine-loaded liposomes. Curr Drug Deliv. 2007;4:89–101.
4. Celano M, Calvagno MG, Bulotta S, Paolino D, Arturi F, Rotiroti D, et al. Cytotoxic effects of gemcitabine-loaded liposomes in human anaplastic thyroid carcinoma cells. BMC Cancer. 2004; 4(1):63.
5. Celia C, Calvagno MG, Paolino D, Bulotta S, Ventura CA, Russo D, et al. Improved in vitro anti-tumoral activity, intracellular uptake and apoptotic induction of gemcitabine-loaded pegylated unilamellar liposomes. J Nanosci Nanotechnol. 2008;8:2102–13.
6. EliLylli. Summary of product characteristics: gemcitabine. Prescribing information. Indianapolis, USA: EliLylli and Company; 2007.
7. EliLylli. Gemcitabine hydrochloride for injection. Material safety data sheet. 2005.
8. Grabielle-Madelmont C, Perron R. Calorimetric studies on phospholipid-water systems. J Colloid Interface Sci. 1983;95: 483–93.
9. Amenitsch H, Bernstorff S, Kriechbaum M, Lombardo D, Mio H, Rappolt M, et al. Performance and first results of the ELETTRA high-flux beamline for small angle X-ray scattering. J Appl Crystallogr. 1997;30:872–6.
10. Bernstorff S, Amenitsch H, Laggner P. High-throughput asymmetric double-crystal monochromator of the SAXS beamline at ELETTRA. J Synchrotron Radiat. 1998;5:1215–21.
11. Keller G, Lavigne F, Forte L, Andrieux K, Dahim M, Loisel C, et al. DSC and X-ray diffraction coupling. Specifications and applications. J Therm Anal. 1998;51:783–91.
12. Ollivon M, Keller G, Bourgaux C, Kalnin D, Villeneuve P, Lesieur P. DSC and high resolution X-ray diffraction coupling. J Therm Anal Calorim. 2006;85:219–24.
13. Lavigne F, Bourgaux C, Ollivon M. Phase transition of saturated triglycerides. J Phys. 1993;4:137–8.

14. Huang TC, Toraya H, Blanton TN, Wu Y. X-ray powder diffraction analysis of silver behenate, a possible low-angle diffraction standard. J Appl Crystallogr. 1993;26:180–4.
15. Marsh D. CRC handbook of lipid bilayers. FL, USA: CRC Press; 1990.
16. Tristram-Nagle S, Nagle J-F. Lipid bilayers: thermodynamics, structure, fluctuations, and interactions. Chem Phys Lipids. 2004;127:3–14.
17. Tardieu A, Luzzati V, Reman FC. Structure and polymorphism of the hydrocarbon chains of lipids: a study of lecithin-water phases. J Mol Biol. 1973;75:711–33.
18. Ruocco MJ, Shipley GG. Characterization of the sub-transition of hydrated dipalmitoylphosphatidylcholine bilayers. Kinetic, hydratation and structural study. Biochim Biophys Acta (BBA)—Biomembranes. 1982;691:309–20.
19. Janiak MJ, Small DM, Shipley GG. Temperature and compositional dependence of the structure of hydrated Dimyristoyl lecithin. J Biol Chem. 1979;254:6068–78.
20. Janiak MJ, Small DM, Shipley GG. Nature of the thermal pretransition of synthetic phospholipids: dimyristoyl- and dipalmitoyllecithin. Biochemistry. 1976;15:4575–80.
21. Sun WJ, Suter RM, Knewtson MA, Worthington CR, Tristram-Nagle S, Zhang R, et al. Order and disorder in fully hydrated unoriented bilayers of gel phase dipalmitoylphosphatidylcholine. Phys Rev E. 1994;49:4665–76.
22. Nagle JF, Tristram-Nagle S. Structure of lipid bilayers. Biochim Biophys Acta (BBA)—Biomembranes. 2000;1469:159–95.
23. Binder H, Zschörnig O. The effect of metal cations on the phase behavior and hydration characteristics of phospholipid membranes. Chem Phys Lipids. 2002;115:39–61.
24. Pabst G, Hodzic A, Strancar J, Danner S, Rappolt M, Laggner P. Rigidification of Neutral Lipid Bilayers in the Presence of Salts. Biophys J. 2007;93:2688–96.
25. Brandenburg K, Garidel P, Howe J, Andrä J, Hawkins L, Koch MHJ, et al. What can calorimetry tell us about changes of three-dimensional aggregate structures of phospholipids and glycolipids? Thermochim Acta. 2006;445:133–45.
26. Claessens MMAE, van Oort BF, Leermakers FAM, Hoekstra FA, Cohen Stuart MA. Charged lipid vesicles: effects of salts on bending rigidity, stability, and size. Biophys J. 2004;87:3882–93.
27. Yue B, Huang C-Y, Nieh M-P, Glinka CJ, Katsaras J. Highly stable phospholipid unilamellar vesicles from spontaneous vesiculation: a DLS ans SANS study. J Phys Chem B. 2005;109:609–16.
28. Hauser H. Some aspects of the phase behaviour of charged lipids. Biochim Biophys Acta (BBA)—Biomembranes. 1984;772:37.
29. Nagle J-F, Zhang R, Tristram-Nagle S, Sun W, Petrache HI, Suter RM. X-ray structure determination of fully hydrated Lα phase dipalmitoylphosphatidylcholine bilayers. Biophys J. 1996;70:1419–31.